# TEMPERATURE FIELD OF CONCRETE IN WINTER CONSTRUCTION: FINITE ELEMENT MODELING AND PARAMETRIC STUDY

**WEICHAO YING, GE ZHANG, YINGZI YANG***
*School of Civil Engineering, Harbin Institute of Technology, NO. 73, Huanghe Road, Nangang District, Harbin 150090, China.*

***In winter construction, it is of crucial importance to predict the temperature field of concrete, to avoid frost damage, control the temperature gradient, and ensure the construction quality of concrete. In this study, a modified finite element model (FEM) considering the characteristics of winter construction was proposed to predict the temperature field of concrete. The freezing process of free water and the heat release of hydration varied with concrete temperature was involved in this model. Then, the temperature histories of two types of concrete placed at different subzero temperatures were monitored experimentally and simulated by using the modified FEM. Good agreement of these results confirms the validity and reliability of this model. Finally, some numerical experiments were performed to explore the effects of engineering parameters on the temperature field of early age concrete by using the validated finite element model. The results show the law of influence of concrete placing temperature and geometry, ambient temperature, and the thickness and thermal conductivity of insulation material on the concrete temperature field.***

***Keywords:*** *Finite Element Analysis; winter construction; temperature field; thermal insulation curing*

## 1. Introduction

When the temperature drops to or is expected to be lower than 4 °C, concrete will enter the winter construction period. The curing time for concrete called protection period needs to be carefully calculated to prevent it from being affected by subzero temperatures, such as frost damage and thermal cracking [1]. Newly placed concrete usually has a high degree of moisture saturation since there is a small amount of mixing water participates in the cement hydration reaction. If early age concrete subjects to cold weather before hardening, the frost heave of free water in the concrete will cause early frost damage to the structure. Moreover, the rapid cooling of concrete surfaces and temperature rise of its interior from cement hydration heat is associated with high-temperature gradient and thermal stresses inside the concrete. Whether the concrete produces a thermal cracking depends on the tensile strength of the concrete at this time. Thus, the combination of frost damage and thermal cracking will reduce the strength, durability and inevitably shorten the service life of the concrete structure [2-4].

To prevent concrete from freezing and cracking damage at an early age, many technical measures are taken to ensure that the concrete is correctly produced, placed and protected during cold weather. Protection requirements are strengthened as the ambient temperature decreases. Monitoring the temperature of concrete in different areas is an essential means to guarantee the effectiveness of protective measures. Typically, the temperature of concrete corners and edges should be monitored since these areas are vulnerable to freezing and usually more challenging to maintain at the required temperature. The internal temperature of concrete should also be monitored to ensure that excessive heating and substantial temperature differences do not occur. Therefore, it is desirable and necessary to measure and record the concrete temperature for ensuring that it achieves the required strength and durability. However, the temperature measurement is usually with substantial equipment investment, complicated operation and longer analysis process in practical construction. To obtain the temperature history of the whole concrete member, people embedded plenty of expendable thermistors and thermocouples. Some electronic data loggers are needed to track temperature data on the site until the end of the protection period. Due to these disadvantages, such as high cost, complicated operation and time consuming, developing the prospective temperature prediction methods before construction is not only critical but also beneficial in designing winter construction schemes and reducing cost.

At first, B. G. Scramtaev established the static heat balance equation based on the stable heat transfer theory, and this equation could be used to calculate the concrete temperature in winter construction [5]. This method approximately estimates the average temperature of concrete and the time for its temperature drop to 0 °C with different empirical formulas. Nevertheless, there exists a substantial deviation from the actual monitored results. Subsequently, other researchers proposed

* Autor corespondent/*Corresponding author*,
E-mail: yzyang@hit.edu.cn

some revised equations based on this empirical formula, but there was no considerable breakthrough in theory [6-8]. Until 1981, Wu and Deng proposed a new dynamic thermal balance equation for cooling temperature calculation of non-mass concrete based on the unstable heat transfer theory [9], which is generally accepted to replace the stable heat transfer theory. The outstanding advantage of this method is that many factors influencing the concrete cooling process, such as the environment temperature, the placement temperature and even the insulation protection, etc. are included in the temperature calculations. It is worth noting that mass concrete is not suitable for these methods due to the existence of a temperature gradient between its inner and outer parts.

At present, several methods, such as the graphical method of ACI 207.2R, the Portland Cement Association (PCA) method and the Schmidt method, have been used successfully over the years to calculate the temperature rise in mass concrete members [10,11]. The graphical method in ACI 207.1R-96 provides Charts and Tables for the determination of minimum placement temperature and protection period of concrete. The PCA method is only applicable to the concrete member that the minimal dimension longer than 1.8 m, and could not calculate the time for the concrete needed to cool to a specific temperature, let alone provide the quantification information of the structure temperature differences. In the Schmidt method, a simplified numerical solution was developed for the heat transfer process governed by the Fourier law. Compared to the graphical method and PCA method, it is easy to perform the calculation by hand. The above three methods are only appropriate for estimating the temperature rise in mass concrete members and cannot predict the concrete temperature evolution, which needed a tremendous manual work.

To overcome the shortcomings of manual calculation, researchers introduced some numerical simulation methods to calculate the temperature field development of concrete by computer. In 2013, Zahra Najafi and Kaveh Ahangari used multivariate regression and artificial neural networks to predict the temperature field of concrete at normal temperatures [12]. However, this method is complicated to implement since it requires a solid foundation knowledge of computer programming. Thus, it is quite necessary to develop an easy and accurate method for predicting the temperature evolution of concrete.

As the most commonly used numerical method, the finite element method (FEM) can simulate the temperature field of concrete structure such as bridge [13], dam [14,15], road paving [16], foundation [17], etc. Meanwhile, it accurately evaluates and analyses the impact degree of various conditions, including placing process, environmental temperature, initial temperature, mix proportion, hydration heat, insulation measures, etc., during the construction. Moreover, some scholars present the results of the thermal stress field induced by the temperature field and predict whether the temperature crack will occur or not at an early age [18-21]. Most of these researches focus on mass concrete at a normal temperature, which always has risks such as thermal cracking or delayed ettringite formation. The effects of hydration heat and cooling pipe system on the maximum temperature rise and temperature difference of concrete structure are considered seriously in those finite element analyses (FEA) models.

Compared to the proposed FEA model used to simulate the concrete temperature field of conventional construction, the FEA model used for that of winter construction usually needs to consider more aspects. On the one hand, specific protection methods, such as covering the concrete with insulating materials, building enclosures, and intermittent using heaters, are often adopted to satisfy the minimum winter construction requirements. These protection methods would significantly influence the heat transfer process between inside concrete and exterior environment. For example, as the most commonly used protection method, applying insulation materials could significantly improve the heat retention capacity of concrete structures [22,23]. On the other hand, when the temperature is below 0 $^{o}$C, most of the free water that exists in the capillary pores will turn into ice [24]. The exothermic process of water phase change would slightly slow down the cooling rate of concrete and makes the whole analysis process nonlinear. Until now, there is a considerable knowledge gap in predicting the temperature field of concrete in winter construction in the open literature.

In this study, a modified FEA model concerning insulation material, free water freezing process and the modified hydration heat formulation was first established. The software ANSYS was used to simulate the temperature field of concrete. Then, an experimental study is performed to monitor the temperature histories of concrete specimens, which placed in constantly subzero temperature environmental (Refrigerator) and naturally variable subzero temperature environments (Outdoor), respectively. Next, by comparing the simulation results to the experimental results, the reliability and accuracy of the finite element simulation method were proved. Lastly, a series of influencing factors analysis is performed to explore the effect of the size of concrete structure, type of insulation material, the thickness of insulation material, ambient temperature and placement temperature on the temperature field of concrete in winter construction. The analysis results are helpful in designing the winter construction scheme with energy-saving and environmental protection.

### *1.1. Modified finite element model*

Of the models mainly used for normal temperature construction, the established governing equation for heat conduction can achieve the best balance between precision and efficiency. However, the difficulty in predicting the temperature field of concrete in winter is to consider the effect of the freezing process of water below zero and the changing concrete temperature on the heat release from hydration. Otherwise, it would decrease the prediction precision of the temperature field and make it challenging to design the winter construction scheme. In this section, the finite element model was modified by incorporating the thermal phase-change formula and introducing the modified equation of the heat released by cement hydration.

## 2.Thermal modeling

### *2.1.Heat conduction equation*

The essence of temperature field calculation in concrete is to solve the heat conduction equation under specific boundary conditions and initial conditions. Combined the first law of thermodynamics (which indicates energy conservation) with Fourier's law, and specializing it into a differential control volume, it is easy to derive the heat conduction equation:

$$\rho c\dot{T} = \nabla(\lambda \nabla T) + q \quad (1)$$

where $\rho$ is the density of the concrete (kg/m$^3$); $c$ is the specific heat ( J/(kg·K) ); $\lambda$ is the thermal conductivity (W/(m·K)); $T$ is the temperature (K), and $q$ is the heat generation rate per unit volume J/(m$^3$·s).

### *2.2.Boundary conditions*

The initial condition of uniform temperature distribution throughout the concrete at time $t = 0$ can be applied as:

$$T|_V(x, y, z, 0) = T_P \quad (2)$$

where $T_P$ is the placing temperature of the concrete.

The boundary condition of thermal analysis at a given structure may be summarized with three simplified forms (Eqs. (3), (4) and (5)):

- Specified temperatures acting over surface $S_1$:

$$T|_{s_1} = T_w \text{ or } T|_{s_1} = f(x, y, z, t) \quad (3)$$

- Specified heat flows acting surface $S_2$:

$$Q_n = -\lambda\frac{\partial T}{\partial n}|_{s_2} = Q_w \text{ or } Q_n = -\lambda\frac{\partial T}{\partial n}|_{s_2} = g(x, y, z, t) \quad (4)$$

- Specified convection surfaces acting over surface $S_3$ (Newton's law of cooling):

$$Q_n = -\lambda\frac{\partial T}{\partial n}|_{s_3} = h(T - T_{s_3}) \quad (5)$$

### *2.3.Discretization and finite element analysis*

As stated before, the variable $T$ is allowed to vary in both space and time. This dependency is separated as:

$$T = [N]^T \cdot \{T_e\} \quad (6)$$

where $[N]$ is the element shape functions and $\{T_e\}$ is the nodal temperature vector of the element.

Combining the stiffness matrix of all involved elements, the total stiffness matrix of the structure is obtained. Through taking the extreme value of functional variation for transient heat conduction (Eq. (7)) ($\left\{\frac{\partial \Pi}{\partial T}\right\} = \{0\}$), the finite element governing equation is given (Eq. (8)).

$$\Pi = \int_V \left\{\frac{\lambda}{2}(\nabla T)^2 - qT + c\rho T\dot{T}\right\}\mathrm{dV} - \int_{s_2} Q_w T\mathrm{dA} + \frac{1}{2}\int_{s_3} h(T_{s_3} - \frac{1}{2}T)\, T\mathrm{dA} \quad (7)$$

$$[C]\{\dot{T}\} + [K]\{T\} = \{Q\} \quad (8)$$

where $[K]$ is the conductivity matrix; $[C]$ is the specific heat matrix; $\{Q\}$ is the applied heat flows and $\{T\}$ is the vector of nodal temperatures, respectively.

## 3.Latent heat modeling

In the process of phase change analysis, the specific heat matrix $[C]$, which is expressed as Eq. (7), should consider the latent heat of the element phase change.

$$[C] = \int \rho c[N]^T[N]\mathrm{d}V \quad (9)$$

A direct calculation can be expected to lead to satisfactory numerical integrations only if the $\rho c$, $\lambda$ and $q$ versus temperature curves do not present sharp peaks. If instead, a phase change process is considered, calculated results are likely not convergent [25]. When the temperature approaches the phase change temperature, the equivalent heat capacity tends to the Dirac $\delta$ function and, therefore, cannot be satisfactorily represented across the peak by a smooth function. A more appropriate averaging process can be successfully tackled such extreme problems [26].

The latent heat of the phase change process is simulated by an artificial increase in the specific heat. The heat capacity with respect to temperature (enthalpy) is a smooth function of temperature in the phase change zone:

$$H = \int \rho c(T)\mathrm{d}T \quad (10)$$

Therefore, replaced $\rho c$ with $H$ , the heat transfer equation (Eq. (1)) could be transformed into Eq. (10), as follow:

$$\dot{H} = \lambda\nabla^2 T + q \quad (11)$$

The relationship between enthalpy and temperature could be deduced as follows:

$$H = \begin{cases} \rho c_s(T - T_l) & T < T_s \\ \rho c_s(T_s - T_l) + \rho c^*(T - T_s) & T_s \le T \le T_l \\ \rho c_s(T_s - T_l) + \rho c^*(T_l - T_s) + \rho c_l(T - T_l) & T_l \le T \end{cases} \quad (12)$$

$$c^* = \rho\left(\frac{(c_s + c_l)}{2} + \frac{L}{(T_l - T_s)}\right) \quad (13)$$

where $c_s$ and $c_l$ is the specific heat of solid phase and liquid phase, respectively; $T_s$ and $T_l$ is the critical temperature for solid melting and liquid freezing, respectively; and $L$ is the latent heat for the phase change process.

As for concrete, $T_s$ and $T_l$ of Eq. (13) and (14) are affected by the type and proportion of antifreeze and pore size distribution (usually determined by the age of concrete). Generally, higher content of antifreeze and finer pores distribution result in lower values of $T_s$ and $T_l$.

In order to simplify the Finite Element Model (FEM), we assume that the free water phase and other phases in concrete constitute a whole uniform phase when predicting its temperature field in winter construction. Therefore, the transform equivalent between the latent heat of free water freezing and phase changing of the homogeneous materials can be expressed as Eq. (14).

$$L = L_w \frac{m_w}{m} \tag{14}$$

where $L_w$ and is $L$ the latent heat of phase transformation of water and whole concrete (J/(kg)), respectively; $m_w$ and $m$ is the weight of free water per unit volume concrete and concrete per unit volume (kg/$\mathrm{m}^3$), respectively.

Naturally, the specific heat of the homogeneous materials could be calculated from Eq. (15).

$$c = \frac{c_w m_w + c_o(m - m_w)}{m} \tag{15}$$

where $c_w$ and $c_o$ is the specific heat of free water and other phases in concrete J/(kg·K).

Compared to the weight of whole concrete, the weight of free water usually presents relatively small (generally, $\frac{m_w}{m} < 10\%$ ). Since other phases in concrete have no phase transformation and latent heat caused by the cooling process, the specific heat of whole concrete could presume as a constant value.

$$c = c_s = c_l \tag{16}$$

### *3.1.Internal heat source modeling*

For concrete, the function $q$ of Eq. (1) and Eq. (10) describes the internal heat released rate from cement hydration, which can be generally expressed as follows (Eqs. (17) and (18)):

$$q(\tau) = m(W + kF)Q_\infty e^{-m\tau} \tag{17}$$

$$Q(\tau) = Q_\infty(1 - e^{-m\tau}) \tag{18}$$

where $W$ and $F$ is the cement content and the admixture content per unit volume concrete (kg/m$^3$) respectively; $k$ is the admixture coefficient which is related to the used admixture type; $Q_\infty$ is the total heat generation per unit cement content (J/kg); $m$ is the coefficient of hydration rate.

However, when the concrete temperature below a specific value (subzero), most of the free water in fresh concrete turns into ice. Consequently, the hydration process essentially stops, and there is only a little water to react with the cement. Therefore, in winter construction, it is necessary to consider the influence of freezing point temperature of free water on the cement hydration courses. The modified heat generation equation is easily expressed as follows:

$$q(\tau) = \begin{cases} m(W + kF)Q_\infty e^{-m\tau} & T < T_f \\ 0 & T > T_f \end{cases} \tag{19}$$

where $T_f$ is the freezing point temperature of free water (K).

This equation assumes that the process of cement hydration ceased when its temperature below the freezing point of the liquid phase.

## 4.Experiments and numerical simulation

### *4.1.Verification experiments*

#### *4.1.1.Materials and mix proportion*

The C40 grade concrete was designed in this experiment, and its mixture proportion was shown in Table 1. The cement is P.O.42.5 cement produced by Harbin Yatai Group. The aggregate is composed of natural sand as fine aggregate and gravel as coarse aggregate. The fine aggregate is well-classified zone II sand with fineness modulus of 2.82 and a density of 2.60 g/cm$^3$. The used coarse aggregate was continuous grading with a maximal grain size of 25 mm, a crushing index of 4.8 % and an apparent density of 2.65 g/cm$^3$. The polycarboxylate superplasticizer, sodium nitrite, and air-entraining agent were used in this experiment. These admixtures can improve the workability, optimize the pore size distribution and reduce the frost heaving stress of concrete to a certain extent.

To explore the influence of water freezing on the cooling process of concrete, we designed two mix proportions and two curing conditions at subzero temperatures. As shown in Table 1, the difference between the two mixes is that Mix2 mixed with 3% sodium nitrite and Mix1 not. Mix1's concrete is wrapped with insulation material and goes directly into the refrigerator at constant -15°C, while Mix2 is placed outdoor with an ambient environment temperature ranging from -8°C to -25°C. The purpose of this test scheme is to cover the conventional working conditions of concrete during winter construction.

#### *4.1.2.Specimen fabrication and data collecting*

An experimental monitoring campaign for measuring early-age temperature was carried out on two mix concrete specimens. The geometry dimension of the concrete specimen is 100 mm × 100 mm × 100 mm . At subzero temperature, if the specimen without corresponding protection measures, the early age hydration process of cement and strength development of concrete would be hindered and concrete would suffer from frost damage. Therefore, a layer of expanded polystyrene (EPS) board was selected as an insulation material. All concrete specimens were insulated and wrapped with 17mm thick plywood formwork used as a mold for fresh concrete, and 50mm EPS board used as an insulation material, as shown in Fig. 1

**Table 1**

Mix proportion of concrete

| Material type | Unit weight value (kg/m$^3$) | |
|---|---|---|
| | Mix 1 | Mix 2 |
| P.O.42.5 cement | 380 | 380 |
| Slag | 60 | 60 |
| Water | 167 | 167 |
| Coarse aggregate | 1069 | 1069 |
| Fine aggregate | 774 | 774 |
| Superplasticizer | 4.84 | 4.84 |
| Air-entraining agent | 0.088 | 0.088 |
| Anti-freezing admixture | 0 | 3% |

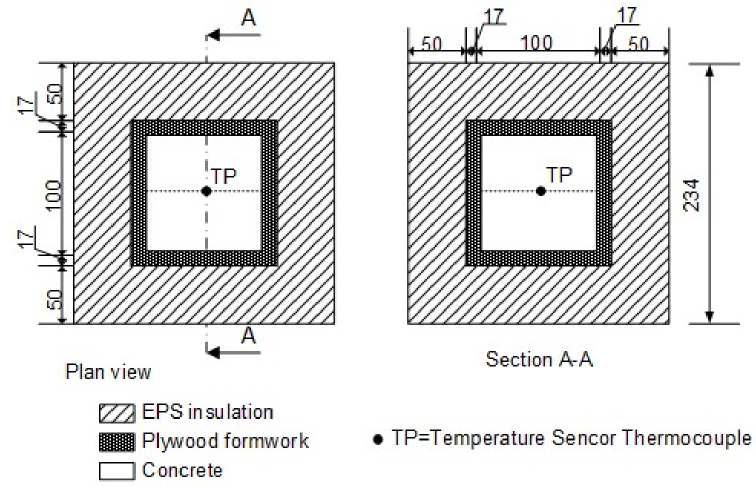


Fig. 1 - Experimental set-up.

The specimens were cast and wrapped by EPS board at room temperature and then instantly placed into the refrigerator of -15 °C and outdoors. Type T copper-constantan thermocouple with high precision was embedded into the center of the specimen to monitor the temperature profile inside the concrete, which arrangement is also shown in Fig. 1. At the same time, two thermocouples monitor the temperature history of the refrigerator and the outdoor environment, respectively. The temperature of two specimens was recorded every 1 minute with a TRM-WD120 automatic temperature for 72 h.

### 4.2.Numerical model

#### 4.2.1.Computational parameters

The total heat generation per unit cement content ( $Q_\infty$ ) is related to the cement type. According to reference [27], the value of $Q_\infty$ for the P.O.42.5 cement used in this experiment is chosen as 461000 J/kg . The hydration rate $m$ mainly determined by the initial temperature of concrete. In this experiment, the $m$ is selected as 0.3 [27]. The specimen of Mix1 placed in the -15 °C refrigerator is at a natural convection state. Another specimen of Mix2 is at a forced convection state. The surface heat transfer coefficient of these two specimens that calculated from the empirical formula is 10.25 W/(m$^2$·K) and 16.96 W/(m$^2$·K), respectively [28]. According to the phase change temperature of the water, $T_s$ and $T_l$ were selected as -1 °C and 0 °C. The free water content in the hydrating cement paste, which is defined as the mass of free water divided by the sum of initial masses of cement and water, was 0.2 from 6 h to 28 h after mixing [29]. Then $\frac{m_w}{m} = 4.96\%$ , and naturally, $L = 16\text{kJ/m}^3$ could be easily deduced. Other thermal parameters that required for the finite element analysis are listed in Table 2, where the specific heat, thermal conductivity, and density of the concrete, EPS, and plywood was referred from the GB50496-2009 Code [27] or measured by proper equipment.

#### 4.2.2.Finite element modeling

A commercial finite element analysis software ANSYS was used to analyze the transient temperature field of concrete. After considering the three-dimensional symmetry of the specimen, the one-eighth size of the specimen was selected for finite element analysis. The three-dimensional thermal element Solid 70, which has eight nodes

**Table 2**

Thermal parameters of the materials for the FEM model

| Material type | Density (kg/m$^3$) | Specific heat (J/(kg·K)) | Thermal conductivity (W/(m·K)) |
|---|---|---|---|
| Concrete | 2450 | 970 | 2.600 |
| EPS | 32 | 1380 | 0.038 |
| Plywood | 750 | 1134 | 0.150 |

and one degree of freedom for each node, was elected. This element can be used for three-dimensional static or transient thermal analysis, and it can also be converted into a structural element for stress and strain field calculation.

The finite element model consists of a thermal insulation layer (EPS board), plywood mold and concrete. The thermal insulation layer and wood mold layer are non-topological geometries that cannot be meshed by mapped meshing and sweeping meshing. In order to reduce the computational scale and ensure the accuracy of calculation results, we used free meshes with different densities for EPS board, wood mold, and concrete, respectively. The meshed finite element model is consisted of 2804 nodes and 13779 elements, as shown in Fig. 2.

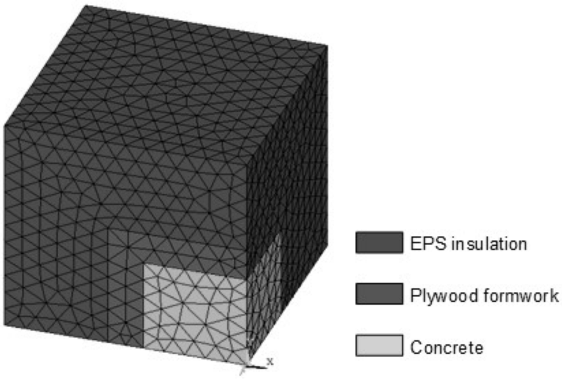


Fig. 2 - Meshed finite element model (One-eighth of real size).

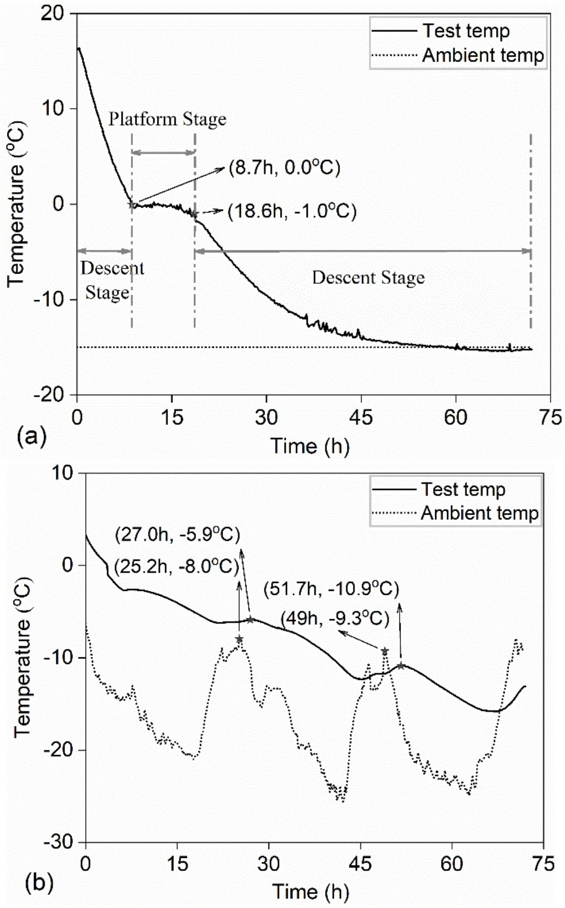


**Fig. 3 -** Test temperature-time history curves. (a) Mix 1, (b) Mix 2.

## 5.Results and discussion

### *5.1.Experimental results*

The temperature-time histories of two specimens placed in the refrigerator and at the outdoor are shown in Fig. 3(a) and Fig. 3(b), respectively. In Fig. 3(a), the center temperature of the Mix1 specimen begins to decrease due to the lower ambient temperature. It takes 8 hours for the center temperature of the concrete to drop to 0 °C. Since then, a large amount of free water that is not involved in the hydration reaction of cement freezes and continuously releases heat, preventing a further reduction of concrete temperature. The phase change process lasts about 10 hours. After all the free water freezes, it is reasonable to assume that the cement hydration reaction has stopped, and naturally, the hydration heat stops generating. Subsequently, the temperature of concrete begins to drop again. With time prolongs, the rate of the temperature decline is gradually reduced. At 60 h, the temperature drops to -15 °C, which is the set temperature of the refrigerator.

The temperature-time history of the specimens cured at the outdoors can be seen in Fig. 3(b). Because the anti-freezing agent in Mix2 can prevent the water from freezing at low temperatures, there is no phase change in the liquid phase of concrete, and cement can continue to hydrate to some degree at a negative temperature. Therefore, there is no distinct temperature platform on the cooling curve similar to the 0 °C range in the Mix1 specimen. Although temperatures rise during the day and decrease at night, the temperature of concrete generally shows a downward trend with small fluctuations. It is worth noting that near the highest temperature of the day (approximately 24 hours, 48 h and 72 h of the curve), the temperature at the core of the specimen increased slightly and it lasted approximately 6 hours per day. On the first and second days after concrete casting, the high ambient temperatures peak about -8 °C at 25 h and 49 h, while the high concrete temperatures peak at 5 °C and -12 °C, respectively at 27 h and 51 h. It can be seen that the internal temperature change of concrete lags behind obviously.

### *5.2.Verification for numerical simulation*

The temperature-time histories of the concrete center are derived and compared with the experiment results, as shown in Fig. 4. From Fig. 4(a), it can be seen that, at the very beginning, the Mix1 specimen's cooling rate in the simulated results is smaller than that in the experiment. That may be because the cement hydration heat formula adopted in this simulation model does not consider the induction period of cement hydration. As time increases, both the numerically simulated and the monitored temperatures decrease rapidly to 0 °C. Both of them all go through a temperature platform period and then continue to decline until they

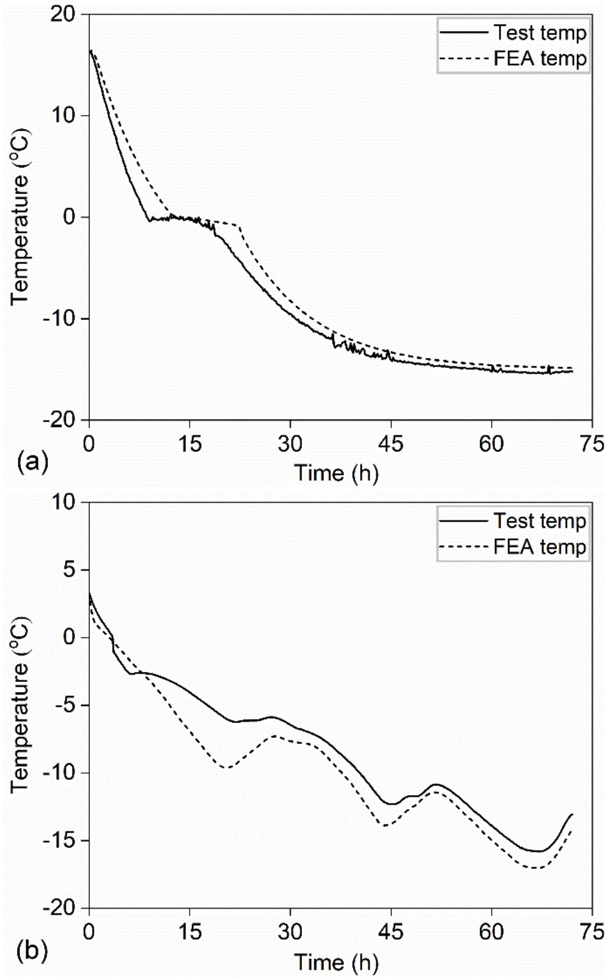


Fig. 4 - Comparison between the monitored temperature and the numerical simulation results.(a) Specimen Mix 1 in the refrigerator, (b) Specimen Mix 2 in outdoor.

balanced with the ambient temperature. In most cases, the deviation between the monitored and simulated temperature is less than 1 °C.

The temperature-time histories of the Mix2 specimens placed outdoor are also compared with the monitored results, as shown in Fig. 4(b). The measured temperature first drops rapidly, and then go through a flattening period, while the simulated temperature drops continuously and slowly. The maximum temperature deviation between simulated and monitored results is 3.79 °C and occurs at 19.7 h. As time increases, the temperature-time history curves of the monitored and simulated have the same trend and are consistent with each other in general. The deviation between the two is less than 2 °C at most of the time. Because the simulated temperature is lower than the measured temperature, it is safe and beneficial in preventing frost damage and designing a construction scheme in winter. Although there are some temperature differences between the tested and the FEA simulated, the accuracy and reliability of the temperature-time curve of concrete obtained by ANSYS simulation can be accepted in winter construction.

## 6.Parametric analysis

### *6.1.Taguchi method and simulated experimental design*

The Taguchi method utilizes orthogonal arrays from the design of experiments theory to study a large number of variables with a relatively small number of tests. Using orthogonal arrays significantly reduces the number of experimental configurations to be researched. Meanwhile, the conclusions induced from small scale experiments are valid over the entire experimental region spanned by the control factors.

The influence of several typical factors on temperature field development of concrete in winter construction is investigated in this section. They are described as follow:

- Placement temperature of concrete ($T_P$);
- Environment temperature ($T_E$);
- Insulation thermal conductivity ($\lambda_I$);
- Insulation thickness ($D_I$);
- Concrete size ($D_C$);

The orthogonal array (OA) is devised, and the variation levels of the considered factors are shown in Table 3. To match with the actual winter construction, we design the placing temperature of concrete and environment temperature form 5 °C to 20 °C and -5 °C to -20 °C, respectively. In this part, $L_{16}(4^5)$ OA is used, and other factors sets are defined in Table 4.

### *6.2.Simulation results and discussion*

When the corners of the early age concrete cool down to subzero temperature, the freezing of free water will cause local damage to the concrete. If the central part of the concrete subjects to subzero temperature, the entire concrete specimen will be vulnerable to frost damage. Therefore, two parameters including the time required to cool the corner of concrete to below zero ($\tau_n$) and the time required to cool the center of concrete to below zero ($\tau_t$) are selected as the dependent variables to evaluate the impact of various factors on the freezing damage of concrete. Besides, the rapid cooling of concrete surfaces causes a considerable temperature difference between the outside and inside of the concrete structure, which can lead to thermal cracking in concrete. Thus, the maximum temperature difference in early age concrete ($T_d$) is chosen as another dependent variable to assess the influence of the above factors on the thermal cracking of concrete. The results of $\tau_n$, $\tau_t$ and $T_d$ under the action of different factors are presented in Table 5.

The optimized level for each factor was determined when maximizing $\tau_n$, $\tau_t$ and minimizing $T_d$. The interactive effects of the factors are not considered because all the factors are dependently set in the finite element model. A commercial software SPSS is utilized to analyze the obtained simulation data and the best possible construction scheme design of the concrete structure can be

**Table 3**

Factors and their variation levels

| Factors | Levels | | | |
|---|---|---|---|---|
| | 1 | 2 | 3 | 4 |
| $T_P$ (oC) | 5 | 10 | 15 | 20 |
| $T_E$ (oC) | -5 | -10 | -15 | -20 |
| $\lambda_I$ (W/(m·K)) | 0.02 | 0.03 | 0.04 | 0.05 |
| $D_I$ (mm) | 30 | 40 | 50 | 60 |
| $D_C$ (mm) | 100 | 200 | 300 | 400 |

**Table 4**

Details of the setting factors

| Trial no. | $T_P$ (oC) | $T_E$ (oC) | $\lambda_I$ (W/(m·K)) | $D_I$ (mm) | $D_C$ (mm) |
|---|---|---|---|---|---|
| 1 | 5 | -5 | 0.02 | 30 | 100 |
| 2 | 5 | -10 | 0.05 | 50 | 300 |
| 3 | 5 | -15 | 0.03 | 60 | 400 |
| 4 | 5 | -20 | 0.04 | 40 | 200 |
| 5 | 10 | -5 | 0.04 | 60 | 300 |
| 6 | 10 | -10 | 0.03 | 40 | 100 |
| 7 | 10 | -15 | 0.05 | 30 | 200 |
| 8 | 10 | -20 | 0.02 | 50 | 400 |
| 9 | 15 | -5 | 0.05 | 40 | 400 |
| 10 | 15 | -10 | 0.02 | 60 | 200 |
| 11 | 15 | -15 | 0.04 | 50 | 100 |
| 12 | 15 | -20 | 0.03 | 30 | 300 |
| 13 | 20 | -5 | 0.03 | 50 | 200 |
| 14 | 20 | -10 | 0.04 | 30 | 400 |
| 15 | 20 | -15 | 0.02 | 40 | 300 |
| 16 | 20 | -20 | 0.05 | 60 | 100 |

**Table 5**

Characteristic parameters of the concrete temperature field

| Trail no. | $\tau_n$ (h) | $\tau_t$ (h) | $T_d$ (°C) |
|---|---|---|---|
| 1 | 37 | 42 | 0.62 |
| 2 | 76 | 94 | 2.87 |
| 3 | 162 | 179 | 3.61 |
| 4 | 6 | 12 | 2.99 |
| 5 | 184 | 196 | 2.62 |
| 6 | 13 | 14 | 1.18 |
| 7 | 10 | 15 | 3.66 |
| 8 | 171 | 187 | 3.87 |
| 9 | 163 | 184 | 4.78 |
| 10 | 140 | 146 | 1.76 |
| 11 | 9 | 11 | 1.87 |
| 12 | 39 | 53 | 5.16 |
| 13 | 136 | 144 | 2.35 |
| 14 | 102 | 124 | 6.48 |
| 15 | 133 | 144 | 3.58 |
| 16 | 8 | 9 | 2.42 |

determined in terms of the main effect plot graphs from Fig. 5 for $\tau_n$, $\tau_t$ and $T_d$.

Using analysis of variance (ANOVA) technology, the response data given in Table 5 is analyzed to examine the variation of performance in the process of concrete temperature field development. Statistical analysis was performed to determine the statistically significant factors, and the results are presented in Table 6. The contribution ratio was calculated to assess the level of each factor's importance, as shown in Table 6. When the contribution ratio is high, the contribution of the factors to that particular response is more remarkable. Similarly, the lower contribution percent means a small donation caused by this factor.

As can be seen from Fig. 5(a) and Fig. 5(b), the increase in ambient temperature, insulation thickness, and concrete size, extends the time for the concrete corner and center to drop to 0 °C. While lowering the thermal conductivity of the insulation material also reduces the occurrence of early freezing of concrete. The size of concrete is the most influencing factor on $\tau_n$ and $\tau_t$ with 53.7 % and 60.1 % contribution ratio, respectively. The second influencing factor is environment temperature with 16.4 % and 15.3 % contribution ratio, respectively. The effect of placement temperature on $\tau_n$ and $\tau_t$ is the least, with only 2.3 % and 1.7 % contribution ratio. The contribution rank of five factors on time required for concrete resist frost damage can be summarized in Table 6. The optimal conditions for preventing concrete from frost damage are obtained at 20 °C of $T_P$, -5 °C of $T_E$, 0.02 W/(m·K) of $\lambda_I$, 60 mm of $D_I$ and 400 mm of $D_C$ in this study.

The maximum temperature differences between the center and the corner of the concrete of all simulation tests are less than 10 °C. These small temperature differences only give rise to low

**Table 6**

Analysis of variance results of the purpose parameters

| Factor | Statistical parameters | $\tau_n$ | $\tau_t$ | $T_d$ |
|---|---|---|---|---|
| $T_P$ | DF[a] | 3 | 3 | 3 |
| | SSS[b] | 1589.2 | 1355.3 | 3.4 |
| | MS[c] | 529.7 | 451.8 | 1.1 |
| | F characteristics | 1.0 | 1.0 | 1.6 |
| | Contribution (%) | 2.3 | 1.7 | 10.0 |
| $T_E$ | DF | 3 | 3 | 3 |
| | SSS | 11600.7 | 12358.3 | 2.1 |
| | MS | 3866.9 | 4119.4 | 7.0 |
| | F characteristics | 7.3 | 9.1 | 1.0 |
| | Contribution (%) | 16.4 | 15.3 | 6.1 |
| $\lambda_I$ | DF | 3 | 3 | 3 |
| | SSS | 7045.2 | 6646.3 | 2.7 |
| | MS | 2348.4 | 2215.4 | 0.9 |
| | F characteristics | 4.4 | 4.9 | 1.3 |
| | Contribution (%) | 10.0 | 8.2 | 7.9 |
| $D_I$ | DF | 3 | 3 | 3 |
| | SSS | 12484.7 | 11834.8 | 4.6 |
| | MS | 4161.6 | 3944.9 | 1.5 |
| | F characteristics | 7.9 | 8.7 | 2.2 |
| | Contribution (%) | 17.7 | 14.7 | 13.4 |
| $D_C$ | DF | 3 | 3 | 3 |
| | SSS | 37912.7 | 48495.3 | 21.5 |
| | MS | 12637.6 | 16165.1 | 7.2 |
| | F characteristics | 23.9 | 35.8 | 10.3 |
| | Contribution (%) | 53.7 | 60.1 | 62.6 |

[a] Degree of freedom, [b] Sequential sum of square, [c] Mean square (variance)

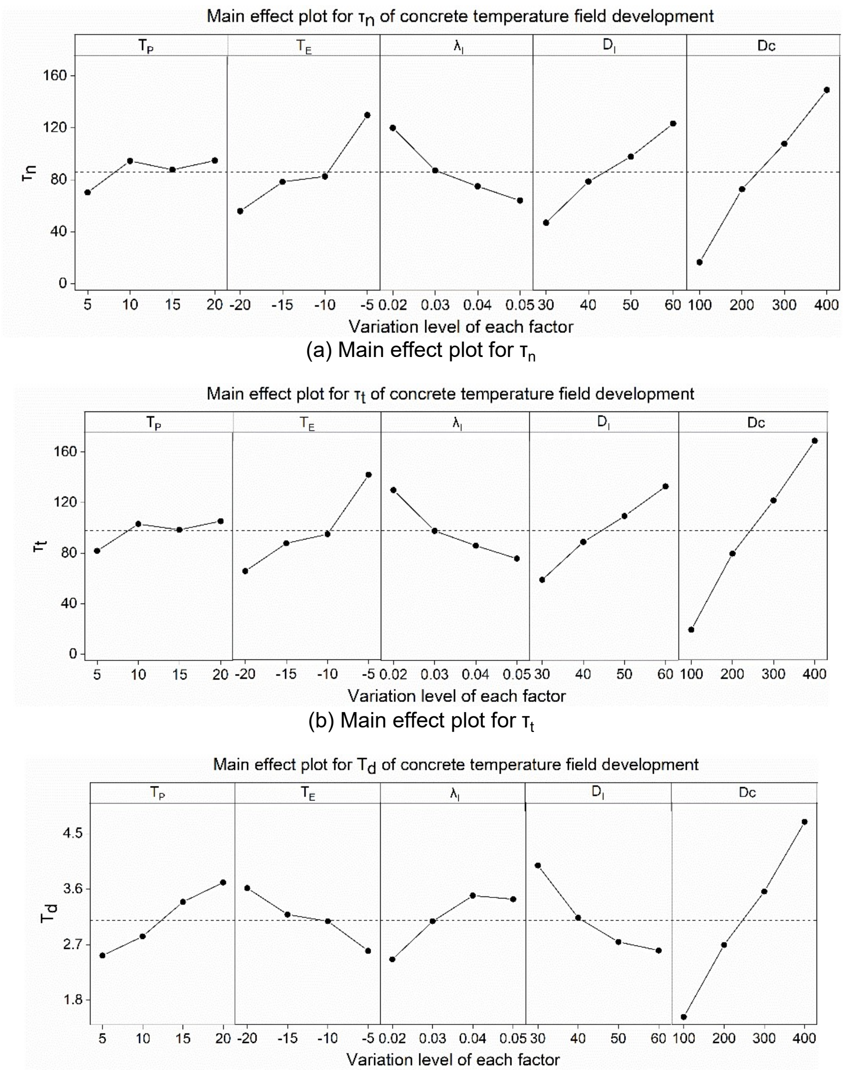


(a) Main effect plot for $\tau_n$

(b) Main effect plot for $\tau_t$

(c) Main effect plot for $T_d$

Fig. 5 - Main effect plot.

thermal stress, which could not cause thermal cracking to a concrete structure. However, comparing with the maximum concrete size chosen in this study (400 mm × 400 mm × 400 mm), the size of the actual structure constructed in winter, such as bridge pier and foundation, usually can reach several meters or even tens of meters. For these structures, rapid cooling of concrete surfaces and temperature rise of concrete interior caused by cement hydration could raise significant temperature differences between the exterior and interior regions of the concrete structure, which made it easily suffer from thermal cracking. Thus, the influence of selected factors on $T_d$ should be discussed in the project application.

When placement temperature, insulation material conductivity, and concrete size are increased in the simulation tests, the maximum temperature difference is enlarged. However, increasing the environment temperature and insulation thickness could decrease the maximum temperature difference in different regions of the concrete. Concrete size is the most effective and dominant factor on $T_d$, up to 62.6 % contribution ratio. The rank of their contribution ratio on $T_d$ is: 62.6 % of $D_C$, 13.4 % of $D_I$, 10.0 % of $T_P$, 7.9 % of $\lambda_I$ and 6.1 % of $T_E$. The optimal simulation results for a minimum temperature difference of concrete are 5 °C of $T_P$, -5 °C of $T_E$, 0.02 W/(m·K) of $\lambda_I$, 60 mm of $D_I$ and 100 mm of $D_C$.

According to the analysis of variance results, the geometry of concrete is the dominant factor on the $\tau_n$, $\tau_t$ and $T_d$. The concrete with a larger size is not susceptible to frost damage, but easily has a large temperature difference and then subjects to thermal cracking. As a protection method, insulation plays an important role when used in winter construction. The insulation material with lower thermal conductivity and large thickness has large $\tau_n$, $\tau_t$ and small $T_d$, which means the utilization of insulation could significantly lower the risk of concrete form frost damage and thermal cracking. As can be seen from Table 6, placement temperature at above 5 °C has little effect on the target parameters $\tau_n$, $\tau_t$ and $T_d$. Thus, there is no need to spend too much effort and money to increase it for preventing concrete from early age frost damage and thermal cracking.

### 6.3. Simplified determination of insulation thickness

In order to quickly estimate the required thickness of adopted insulation materials, a simplified formula connecting the insulation thickness and other important factors is determined using the optimal parameter levels obtained from the simulation results listed in Table 5. The fitting formula is suitable for calculating the minimum insulation thickness required for cubic concrete which should be kept away from frost damage until time t

$$D_I = 0.37t + 828.36\lambda_I - 0.26T_P - 1.91T_E - 0.15D_C \qquad (20)$$

where t is the aiming initial frost time of concrete (h); $\lambda_I$ is the thermal conductivity of selected insulation materials; $T_P$ is the placement temperature of concrete; $T_E$ is the environmental temperature; $D_C$ is the size of concrete (side length of the cube).

The needed thickness of the insulation layer can be estimated by incorporating the parameters as mentioned above into Eq. (20). For example, when t = 72 h, $\lambda_I$ = 0.03 W/(m·K), $T_P$ = 15 °C, $T_E$ = -20 °C, and $D_C$ = 200 mm, the estimated insulation thickness $D_I$ = 56 mm can be quickly obtained and was highly consistent with that extracted from the simulation experiments.

## 7. Conclusions

In this paper, the temperature-time history curves for the two mixed concrete placed at different environment temperatures were monitored experimentally and simulated numerically. The main conclusions extracted from this research are as follows:

(1) The established finite element model for in-site concrete considers not only the insulation material but also the freezing process of free water and the changes in hydration heat release with concrete temperature, which commonly happened in winter construction. The new governing equation of heat transfer was improved by incorporating the thermal phase-change formula and the modified equation of the heat released by cement hydration. The model enables a broader scope of application in winter construction.

(2) The monitored temperatures of concrete placed at a constantly subzero temperature environment and naturally variable subzero temperature environment are in good agreement with the simulated ones. Therefore, the numerical simulation model proposed in this study is feasible and reliable for predicting the temperature field of concrete in cold weather concreting.

(3) The influence of several engineering factors on the temperature field of concrete in winter construction is investigated using the Taguchi method. The parametric analysis results show that the concrete size is the dominant factor in affecting the development process of concrete temperature. The concrete with a larger size is not susceptible to frost damage but easily subjects to thermal cracking. As a protection method, the lower thermal conductivity and the larger thickness of insulation material, the safer the concrete winter construction. Lastly, there is no need to spend too much effort and money to increase the placement temperature, which has little effect on the concrete thermal behavior.

Eventually, the scientific determination of the minimum insulation thickness of cubic concrete was realized.

In a word, for concrete constructed in winter, by simulating the temperature field of concrete with the finite element method before construction, the optimal design of thermal conductivity and thickness of insulation material can be obtained, which can significantly reduce the risk of concrete form frost damage and thermal cracking.

***Data Availability Statement***

*Some or all data, models, or code that support the findings of this study are available from the corresponding author upon reasonable request.*

***Acknowledgements***

*The financial support from National Key R&D Program of China (No. 2017YFB0309901) and its Provincial funding (No. GX18A025) for current research is gratefully acknowledged.*

**REFERENCES**

[1] ACI 306R-10, Guide to cold weather concreting, ACI committee 306, American Concrete Institute, 2010.
[2] H. Cai, X. Liu, Freeze-thaw durability of concrete: ice formation process in pores, Cement and Concrete Research 1998, **28**(9), 1281-1287.
[3] S.L. Cha, S.S. Jin, G.G. An, et al. A prediction approach of concrete properties at early ages by using a thermal stress device, Construction and Building Materials, 2018, **178**, 120-134.
[4] S.-T. Yi, S.-W. Pae, J.-K. Kim, Minimum curing time prediction of early-age concrete to prevent frost damage, Construction and Building Materials, 2011, **25**(3), 1439-1449.
[5] Concrete construction technology conference of construction engineering department, Concrete construction technology, Beijing architectural engineering press, 1959, 290-299.
[6] Jinming Bai, Construction and thermal calculation of concrete floor with thermal insulation curing method in winter, Construction Technology, 1957, **13**(1), 13-15.
[7] Chunhe Yao, Some opinions on expanding thermal insulation curing method in winter construction, Construction Technology, 1957, **61**(10),12-18.
[8] Lifang Zheng, Some problems of thermal calculation in thermal insulation construction of concrete engineering, Construction Technology, 1957, **24**(12), 21-24.
[9] Zhendong Wu, Research on computational theory of non-bulk concrete thermal insulation cooling, Construction Technology, 1981, **10**(10), 37-41.
[10] K. A. Riding, J. L. Poole, et al., Evaluation of temperature prediction methods for mass concrete members, ACI Materials Journal, 2006, **103**(5), 357-365.
[11] ACI Committee 207, Mass Concrete (ACI 207.1R-96), American Concrete Institute, Farmington Hills, Mich., 1996, 29-37.
[12] Zahra Najafi, Kaveh Ahangari, The Prediction of Concrete Temperature during Curing Using Regression and Artificial Neural Network, Journal of Engineering, 2013, 1-5.
[13] Y. Huang, G. Liu, et al., Experimental and finite element investigations on the temperature field of a massive bridge pier caused by the hydration heat of concrete, Construction & Building Materials, 2018, **192**, 240-252.
[14] X. Liu, C. Guo, B. Chen, Simulation of temperature field for concrete dam based on ANSYS secondary development, International Conference on Electric Technology & Civil Engineering, 2011.
[15] Y.L. Chen, C.J. Wang, S.Y. Li, et al., The effect of construction designs on temperature field of a roller compacted concrete dam — a simulation analysis by a finite element method, Canadian Journal of Civil Engineering, 2011**, 30**(6), 1153-1156.
[16] J.H. Jeong, D.G. Zollinger, P.E., Finite-Element Modeling and Calibration of Temperature Prediction of Hydrating Portland Cement Concrete Pavements, Journal of Materials in Engineering, 2006, **18**(3), 317-324.
[17] J. Wang, S. Yan, Numerical simulation and real-time survey of temperature fields of mass concrete in raft-foundation, Applied Clay Science, 2015, **101**(3), 604-607.
[18] R. Zhong, G. Hou, S. Qiang, An improved composite element method for the simulation of temperature field in massive concrete with embedded cooling pipe, Applied Thermal Engineering, 2017, **124**, 1409-1417.
[19] M. Azenha, R. Faria, D. Ferreira, Identification of early-age concrete temperatures and strains: Monitoring and numerical simulation, Cement and Concrete Composites, 2009, **31**(6), 369-378.
[20] B. Milovanović, D. Mikulić, M. Đurinek, Finite Element Simulation of Temperature and Stress Development in Mass Concrete, International Conference on Computational Technologies in Concrete Structures, 2009.
[21] F. Sheibany, M. Ghaemian, Effects of Environmental Action on Thermal Stress Analysis of Karaj Concrete Arch Dam, Journal of Engineering Mechanics, 2006, **132**(5), 532-544
[22] M. Sugiyama, H. Takamori, et al., Curing method of the winter construction of the housing base concrete, Concrete Journal, 2003, **41**(7), 23-28.
[23] N. Ekrami, A. Garat, A.S. Fung, Thermal Analysis of Insulated Concrete Form (ICF) Walls, Energy Procedia, 2015, **75**, 2150-2156.
[24] E. Kamada, Frost damage of concrete considering freezing point depression of capillary water in hardened cement paste, Bulletin of the Faculty of Engineering, Hokkaido University, 1988, **145**, 53-61.
[25] C. Bonacina, G. Comini, et al., Numerical solution of phase-change problems, International Journal for Heat mass transfer, 1973, **16**, 1825-1832.
[26] G. Comini, S. Del guidice, et al, Finite element solution of nonlinear heat conduction problems with special reference to phase change, International Journal for Numerical Methods in Engineering, 1974, **8**, 613-624.
[27] GB50496-2009, Code for Construction of Mass Concrete, China Planning Press, Beijing, China, 2009.
[28] Xiaoyun Feng, Shuting Tong, Hua Yuan, Fundamentals of Material Engineering, Chemical Industry Press, Beijing, China, 2007.
[29] J. Pavlík, V. Tydlitát, R. Černý, et al., Application of a microwave impulse technique to the measurement of free water content in early hydration stages of cement paste, Cement and Concrete Research, 2003, **33**(1), 93-102.

***************************************************************************************************